J. Min. Metall. Sect. B-Metall. 52 (1) B (2016) 87 - 92

Journal of Mining and Metallurgy, Section B: Metallurgy

# FABRICATION AND CHARACTERIZATION OF SUPERHYDROPHOBIC AND SUPERLIPOPHILIC SILICA NANOFIBERS MATS WITH EXCELLENT HEAT RESISTANCE

**S. Gao[a], H. Watanabe[a], K. Nakane[a*], K. Zhao[b]**

[a]Frontier Fiber Technology and Science, University of Fukui, Fukui, Japan
[b]Department of Materials Science and Engineering, Xi'an University of Technology, Xi'an, Shannxi, China

*(Received 02 March 2015; accepted 02 September 2015)*

***Abstract***

*A kind of silica nanofibers (SNF) mats with superhydrophobicity and superlipophilicity as well as excellent heat resistance, had been prepared by modifying of 1, 1, 1, 3, 3, 3-hexamethyldisilazane on electrospun SNF mats. The effects of heat treatment time on properties of modified SNF mats were investigated by scanning electron microscopy, nitrogen absorption analysis, X-ray photoelectron spectroscopy, and contact angle measurement. With high specific surface area 240.1 $m^2/g$, the optimal modified SNF mat approached water contact angle (WCA) 153.2° and fuel contact angle (FCA) 0°, furthermore, even after annealing by 450 °C in air for 1h , WCA remained at 135.5° and FCA kept at 3.8°, which opened a new way to improve heat resistance of fuel-water filter paper.*

***Keywords:*** *Nanofibers; Poly (vinyl alcohol); Silica; Superhydrophobicity; Superlipophilicity*

## 1. Introduction

Superhydrophobic surface, with water contact angle above 150° and low rolling angle, has been paid much attention on application of fuel-water filtration [1-7]. Water in fuel is one of the major causes of diesel engine maintenance problems. It is inevitable that water may entrain to fuel during transportation, transfer, and storage of fuel. Water in fuel are mainly divided into two kinds, coarse water and emulsified water, with droplet size 180-260 μm and 15-35 μm, respectively [8]. Fuel-water filter paper, commonly used in diesel engine, plays an important role in separating water from fuel in order to protect precision components of engine from corrosion [9-11]. Generally, commercial fuel-water filter paper mainly consists of silicone treated cellulose fibers, which are however readily dehydrated and carbonized as temperature reaches above 110°C leading to the deformation and the ensuing failure of filter paper [12-14].

Compared with cellulose fiber, inorganic fibers have inherent advantages in thermal deformation resistance which are rising to the challenge to filtration application [15-20]. In addition, Electrospinning (ES) is a facile and cost-effective technology to generate nanofibers with extremely high specific surface area which are very suitable for filtration field [21-26]. Many kinds of electrospun superhydrophobic inorganic nanofibers have been obtained with potential applications in filtration [27-30]. Ding et al. reported an approach for developing a superhydrophobic nanofibrous ZnO film surface modified with a simple coating of fluoroalkylsilane [31]. Tang et al. obtained large area superhydrophobic $TiO_2$ membranes with high adhesive forces which were fabricated by ES followed by calcination and surface modification with fluorinated alkyl silane, pointing to selective transportation of liquid droplets [32]. However, the common used modifier fluoroalkylsilanes are very expensive resulting restriction of commercial applications.

In this study, we prepared superhydrophobic and superoleophilic silica nanofibers (SNF) mats with excellent heat resistance by heat treatment of electrospun poly (vinyl alcohol) (PVA)/silica precursor nanofibers obtained by PVA/silica aqueous solution, followed by modification with 1, 1, 1, 3, 3, 3-hexamethyldisilazane (HMDS). Meng et al. prepared a kind of superhydrophobic surface by grafting of octanol on the surface of electrospun silica nanofiber using organic solvents which are harm to environment and make troubles of solvent recovery. Moreover, specific surface area of the modified SNF declined dramatically from 899 $m^2/g$ to 50 $m^2/g$ which is not enough to achieve high filtration efficiency [33]. In our research, surface modifier HMDS is of

* *Corresponding author: nakane@matse.u-fukui.ac.jp*

***DOI:10.2298/JMMB150302026G***

low cost and the byproduct ammonia easy to clean, and substrate silica is also cost-effective and abundant with hydroxyls, moreover, it is environmentally friendly to utilize water as solution in ES [34-37]. Especially, we studied the effect of heating time on porosities of SNF mats in order to reach optimal specific surface area.

## 2. Experiment

### *2.1 Materials*

Poly(vinyl alcohol) (PVA) with 1500 degree of polymerization was obtained from Wako Pure Chemicals Ind., Ltd., Japan. Tetraethyl orthosilicate (TEOS) and hydrochloric acid (HCl) with 36 wt.% concentration were both got from Nacalai Tesque Ind., Ltd., Japan. Hexamethyl disilazane (HMDS) was a kind gift from Shin-Etsu Chemical Co., Ltd., Japan.

### *2.2 Formation of PVA/$SiO_2$ composite nanofibrous mats by electrospinning*

Firstly, PVA (10 wt.%) aqueous solution was prepared. Secondly, transparent silica sol was made by hydrolysis and condensation reaction of TEOS using HCl as a catalyst. Finally, silica sol with proportion of PVA/$SiO_2$ varied from 90/10 wt.% to 50/50 wt.% was added to PVA solution to get spinning solution.

Electrospinning process is as follows: the spinning solution in 2 ml was loaded into a plastic syringe equipped with a needle. The solution extrusion rate was 0.8 ml/h. A voltage of 20 kV was applied to the needle, resulting that PVA/$SiO_2$ composite nanofibrous mats were deposited on the grounded copper collector. The collection distance from the tip of needle to the collector was 15 cm. The obtained PVA/$SiO_2$ composite nanofibrous mats were used as a precursor to form SNF mats.

In our research, PVA/$SiO_2$ precursor nanofibers were prepared from spinning solution at the PVA/$SiO_2$ mass ratio of 70/30 wt.% can obtain well-formed precursor nanofibers by comparison of nanofibers made by PVA/$SiO_2$ ratios from 90/10 wt.% to 50/50 wt.%.

### *2.3 Formation of SNFs by heat-treatment of precursors*

SNF mats can be obtained by heating PVA/$SiO_2$ composite nanofibrous mats at 600ºC for different given time (1 h, 3 h, 5 h, 10 h) in air using a temperature controllable furnace (Nitto Kagaku Co., Ltd., NPC-TD3, Japan).

### *2.4 Formation of superhydrophobic SNF mats by HMDS modification*

Superhydrophobic SNF mats can be prepared by modifying HMDS on basis of silylation reactions between HMDS and hydroxyls of SNF mats, making hydrophobic trimethylsilyl group (TMS, $(CH_3)_3Si$-) graft on the surface of SNF mats instead of hydrophilic hydroxyls group (OH-).

### *2.5 Apparatus and procedure*

The structure of nanofibers was observed with a scanning electron microscope (SEM) (Keyence VE-9800, Japan). Fiber diameter and its standard deviation was estimated with a digitizer on the enlarged SEM images. The change of surface chemical composition before and after modification was shown by X-ray photoelectron (XP) spectroskopy (JEOL Ltd., JPS-9010MCY, Japan). The water or fuel contact angles were measured by video optical contact angles instrument (AST Products, Inc., VCA Optima-XE, USA). Each contact angle was the average value of five determinations. The specific surface area of nanofibrous mats was tested by automated nitrogen adsorption analyzer at -196ºC (Micromeritics Instrument Co., Ltd., TriStar3000, USA).

## 3. Results and Discussion

### *3.1 Surface morphology of modified SNF mats*

Fig. 1 shows SEM images of modified precursor nanofibers and two kinds of modified SNFs formed by heat treatment of 1 h and 10 h. Fiber diameters decrease dramatically from 480 nm of precursor to 355 nm after 1 h heat treatment, which is attributed to thermal decomposition of PVA. Additionally, fiber diameters with 10 h heat treatment are much smaller than those with 1 h, due to sintering which makes silica nanoparticles gather together closer with heating time increasing.

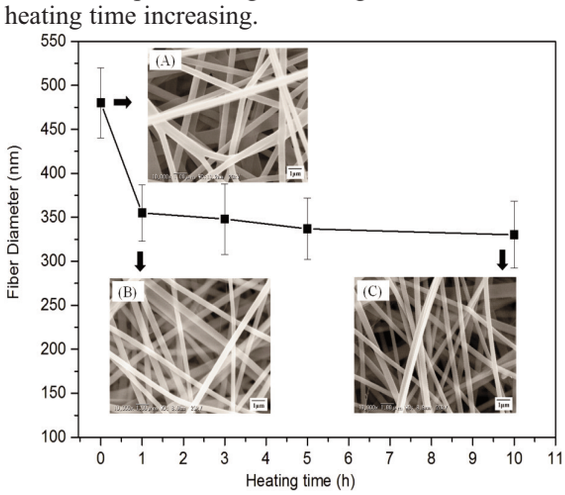


***Figure 1.*** *Effect of heating time on fiber diameter. The insets are corresponding SEM images. (A) PVA/$SiO_2$ precursor nanofibers, (B) $SiO_2$ nanofibers heated for 1 h, (C) $SiO_2$ nanofibers heated for 10 h*

*3.2 Pore characteristics of SNF mats before and after modification*

Fig. 2 shows the effect of heating time on pore characteristics of SNF mats before modification. The specific surface area (SSA) of precursor mat is around 2.1 $m^2/g$ and the average pore diameter (APD) on fibers is 0.3 nm indicating that precursor fiber is nonporous material. However, with 1 h heat treatment to get SNF mats, SSA of SNF mats increases sharply to 260.5 $m^2/g$, meanwhile, APD on fibers grows up to 2.47 nm, due to the thermal decomposition of PVA molecules and the subsequent forming of many mesopores in nanofibers. With increasing heating time from 1 h to 10 h, SSA decrease due to the sintering, however, APD remains around of 2.5 nm, which proves that APD have no direct effect on SSA. But the pore volumes of fibers drop from 0.145 $cm^3/g$ to 0.023 $cm^3/g$ with increasing heating time from 1 h to 10 h, leading to the decline of SSA.

Thus, in order to get SNF mats with high SSA, we selected 1 h as heating time which is the minimum heating time to ensure complete decomposition of PVA. For example, the color of the silica was brown by heating precursor nanofiber for 30 min Furthermore, SSA of modified SNF mats heated by 1h kept at 240.1 $m^2/g$ and APD remains 2.45 nm, which shows excellent porosity for application in filter paper.

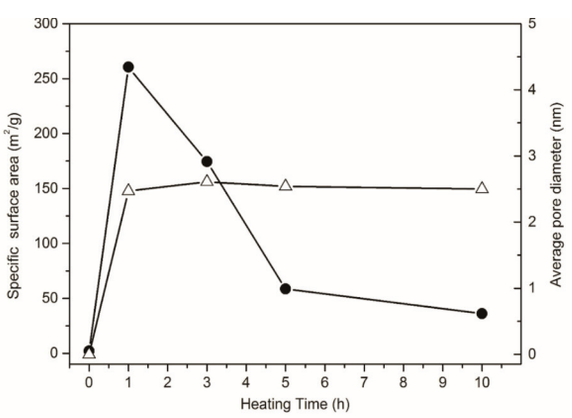


***Figure 2.*** *Effect of heating time on specific surface area and average pore diameter of nanofibers. (● Specific surface area, △ Average pore diameter)*

*3.3 Superhydrophobicity and superlipophilicity of SNF mats modified with HMDS*

As shown in Fig. 3(a), SNF mats possess abundant hydroxyls and capillarity force, leading to superhydrophilicity with water contact angle (WCA) 0° and superlipophilicity with fuel contact angle (FCA) 0°, respectively. When fuel-water mixture droplet went through SNF mats, both water and fuel can pass through the surface.

After HMDS modification, superhydrophobic SNF mats (WCA=153.2°) can be obtained with TMS groups grafted on the surface instead of hydroxyl groups illustrated by Fig.3(b). Meanwhile, superlipophilicity remains (FCA=0°) because of inherent lipophilicity of TMS groups and capillary force of SNF mats. When fuel-water mixture droplet went through modified SNF mats, water can be resisted but fuel can pass through so that water can be separated from fuel.

Fig. 4 shows the XP spectra of carbon 1s electron for (A) as prepared SNF mats (B) HDMS modified SNF mats. New peak around 287.7 eV appears in Fig. 4(B), demonstrating the successful graft of hydrophobic group TMS groups on SNF mats, resulting WCA increases dramatically from superhydrophilicity 0° to superhydrophobicity 153.2°.

In Cassie-Baxter model [38] shown in Fig. 5, surface roughness will prevent water from contacting solid surface completely by forming air bubbles between water and solid. The Cassie-Baxter equation is proposed as Eq.(1) and (2), which can indicate the relationship between the WCA on flat film ($\theta_s$) and on rough surface ($\theta^*$).

$$\cos\theta^* = f_s cos\theta_s + f_g cos\theta_g \quad (1)$$

$$f_s + f_g = 1 \quad (2)$$

Additionally, $f_s$ and $f_g$ are proportions of solid and air on rough surface contacted with water droplet, respectively. Meanwhile, because the WCA of air ($\theta_g$) is 180°, Cassie-Baxter equation can be changed into Eq. (3), in which $f_g$ can be got and reflect the degree of surface roughness.

$$f_g = 1 - \frac{\cos\theta^* + 1}{(1 + \cos\theta_s)} \quad (3)$$

In order to compare with fibrous silica mats, flat silica film was prepared by sol-gel method in which $PVA/SiO_2$=70/30 wt. % and heated at 600ºC for 1h. Fig. 6 shows the SEM image of modified flat silica film and the corresponding WCA of 105.2°, which means $\theta_s$ of silica flat film. The flat film modified by HMDS did not show good hydrophobicity, which is in accordance with the previous report [38] that only with chemical modification and without rough surface, WCA of flat films generally will not exceed 120°. Additionally, $f_g$ can be obtained by Eq. (3) for a given value $\theta_s$ =105$^\delta$.

Fig. 7 shows the effect of heating time on water contact angles and proportion of area contacted with water ($f_g$) on the surface of modified silica nanofibrous mats. It is obvious that water contact

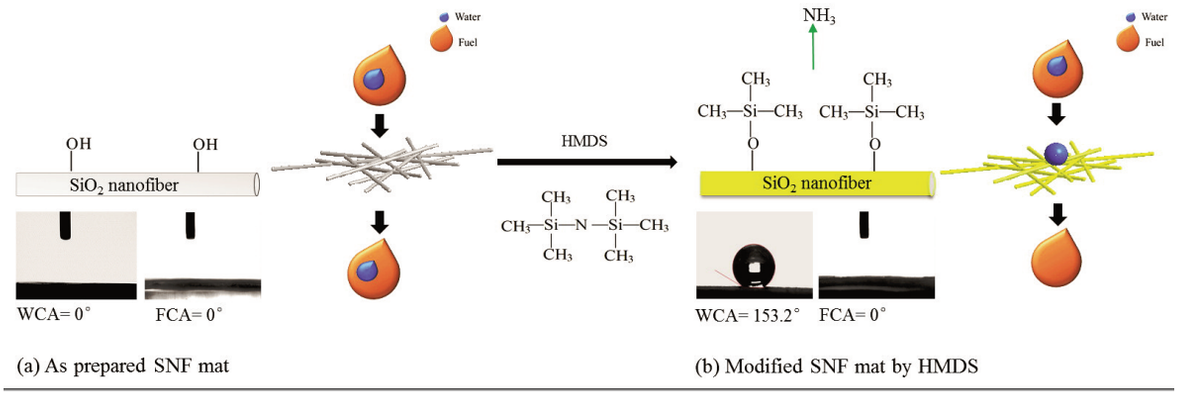


***Figure 3.*** *Schematics of SNF mats before and after modification (a) as- prepared SNF mat (b) modified SNF mat by HMDS. The insects are corresponding pictures of water droplet on mats*

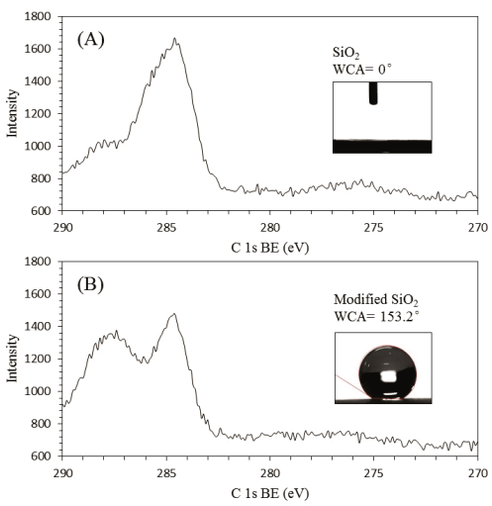


***Figure 4.*** *XP spectra of the surface of (A) as-prepared SNF mats, (B) HMDS modified SNF mats. The insets are corresponding pictures of water droplets on mats*

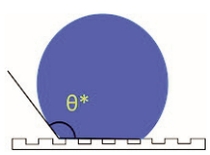


***Figure 5.*** *Schematic diagram of Cassie-Baxter model*

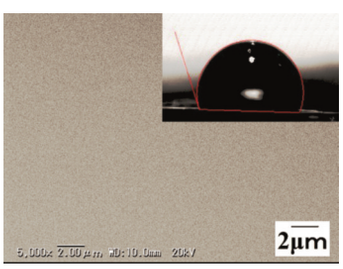


***Figure 6.*** *SEM image of flat $SiO_2$ film modified by HMDS. The inset is the corresponding picture of a water droplet on the film*

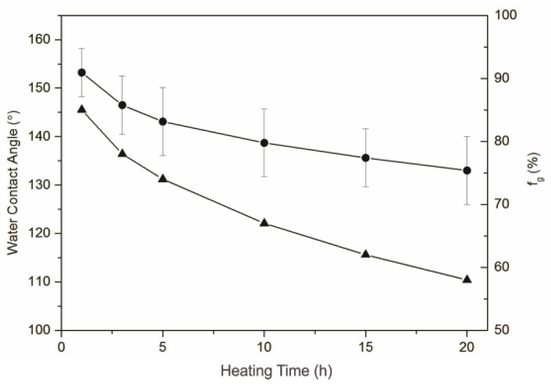


***Figure 7.*** *Effect of heating time on water contact angles (WCA) and ratios of air contacted by water on the surface of modified SNF mats ($f_g$).(● WCA, ▲ $f_g$)*

angles drop from 153.2° to 133° with heating time from 1 h to 20 h in accordance with the decline trend of $f_g$, which means that decrease of surface roughness over heating time leads into decline of hydrophobicity.

In order to be applied in fuel-water filter paper, lipophilicity of modified SNF mats was tested by *n*-dodecane which is the major ingredient in diesel fuel. Fig. 8 shows the process of *n*-dodecane drop contacting with modified SNF mats, during which *n*-dodecane drop can be absorbed rapidly within 0.8 second and fuel contact angel is 0° showing superlipophilic property, as a consequence of capillary force produced by porous structures and inherent lipophilicity of trimethylsilyl group grafted on the surface of SNFs.

### *3.4 Heat resistance of hydrophobicity and lipophilicity of modified SNF mats*

Since the working temperature of diesel filter paper is at the range of 100-150°C, it is very necessary to know the heat resistance temperature of modified SNF mats. The testing experiments were carried out

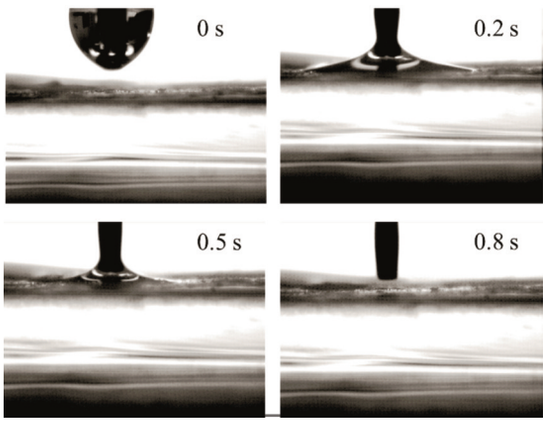


***Figure 8.*** *Process of dodecane drop contacted with modified SNF mat*

by annealing modified SNF mats from 100°C to 550°C for 1 h and measuring the water and fuel contact angles of obtained mats. As shown in Fig. 9(a), water contact angles fall slowly over annealing temperatures from 153.2° to 135.5° below 450°C, however, water contact angle drops down dramatically into 32° once annealing temperature higher than 450°C. When silylated silica is oxidized over 450°C, trimethylsilyl groups (-Si-$(CH_3)_3$) are drastically converted to silanetriol groups (-Si-$(OH)_3$) which leads to sharp decrease of hydrophobicity [40]. Fig. 9(b) reveals the fuel contact angle still kept below 5° even treated by 550°C which shows good heat resistance in lipophilicity.

Therefore, the heat resistance temperature for both hydrophobicity and lipophilicity is estimated to be around 450°C.

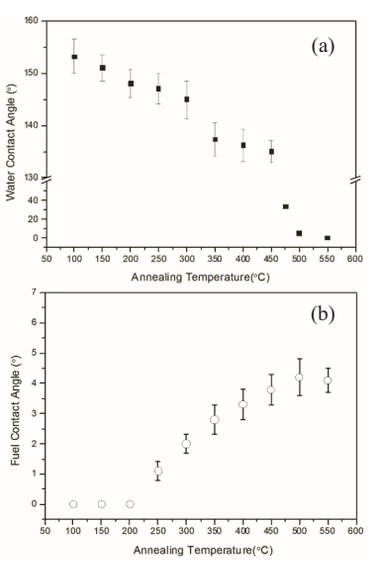


***Figure 9.*** *Heating resistance of modified SNF mats. (a) Effect of annealing temperature on hydrophobicity (b) Effect of annealing temperature on lipophilicity*

## 4. Conclusion

Firstly, PVA/silica hybrid nanofibrous mats were formed by ES using PVA/silica sol aqueous solution as a spinning solution. Then, silica nanofibrous mats were fabricated by heating PVA/silica hybrid nanofibers mats. Finally, hydrophobic nanofibrous mats were formed by modifying surface of silica nanofibrous mats by HMDS. Overall, the optimal modified silica nanofibrous mat obtained by 1 hour heating with high specific surface area 240.1 $m^2/g$ had water contact angle 153.2° and fuel contact angle 0°, as well as heat resistance temperature 450°C.

## References

[1] P. Roach, N.J. Shirtcliffe, M.I. Newton, Soft Matter., 4 (2008) 224-240.

[2] P. Calcagnile, D. Fragouli, I.S. Bayer, G.C. Anyfantis, L. Martiradonna, P.D. Cozzoli, R. Cingolani, A. Athanassiou, ACS nano, 6 (2012) 5413-5419.

[3] Q. Zhu, Q. Pan, F. Liu, J. Phys. Chem. C, 115 (2011) 17464-17470.

[4] W. Zhang, Z. Shi, F. Zhang, X. Liu, J. Jin, L. Jiang, Adv. Mater., 25 (2013) 2071-2076.

[5] F. Zhang, W.B. Zhang, Z. Shi, D. Wang, J. Jin, L. Jiang, Adv. Mater., 25 (2013) 4192-4198.

[6] Z. Shi, W. Zhang, F. Zhang, X. Liu, D. Wang, J. Jin, L. Jiang, Adv. Mater., 25 (2013) 2422-2427.

[7] G. Viswanadam, G.G. Chase, Sep. Purif. Technol., 104 (2013) 81-88.

[8] C. Yang, S. Larsen, S. Wagner, 8th International Filtration Conference, San Antonio, America, 2007, p. 1-5.

[9] O. Armas, R. Ballesteros, F. Martos, J. Agudelo, Fuel, 84 (2005) 1011-1018.

[10] W. Stone, G. Bessee, C. Stanfel, SAE Int. J. Fuel Lubricants, 2 (1) (2009) 317–323.

[11] I. Atadashi, M. Aroua, A.A. Aziz, Renew Sust. Energ. Rev., 14 (2010) 1999-2008.

[12] J. Scheirs, G. Camino, W. Tumiatti, Eur. Polym. J., 37 (2001) 933-942.

[13] V. Mamleev, S. Bourbigot, J. Yvon, J. Anal. Appl. Pyrol., 80 (2007) 151-165.

[14] D. Shen, S. Gu, Bioresource Technol, 100 (2009) 6496-6504.

[15] J. Adler, Int J. Appl. Ceram. Tec., 2 (2005) 429-439.

[16] X.B. Ke, H.Y. Zhu, X.P. Gao, J.W. Liu, Z.F. Zheng, Adv. Mater., 19 (2007) 785-790.

[17] D. Yang, B. Paul, W. Xu, Y. Yuan, E. Liu, X. Ke, R.M. Wellard, C. Guo, Y. Xu, Y. Sun, H. Zhu, Water Res., 44 (2010) 741-750.

[18] Y. Chen, Z. Xue, N. Liu, F. Lu, Y. Cao, Z. Sun, L. Feng, RSC Advances, 4 (2014) 11447-11450.

[19] M. Krissanasaeranee, T. Vongsetskul, R. Rangkupan, P. Supaphol, S. Wongkasemjit, J. Am. Ceram. Soc., 91 (2008) 2830-2835.

[20] X. Huang, J. Song, C. Bai, R. Zhang, M. Zhou, J. Min. Metall. Sect. B-Metall., 51 (2015) 33-40.

[21] R. Gopal, S. Kaur, Z. Ma, C. Chan, S. Ramakrishna, T.

Matsuura, J. Membrane. Sci., 281 (2006) 581-586.

[22] A. Greiner, J.H. Wendorff, Angew. Chem. Int. Ed., 46 (2007) 5670-5703.

[23] R. Barhate, S. Ramakrishna, J. Membrane. Sci., 296 (2007) 1-8.

[24] S. Ramakrishna, R. Jose, P. Archana, A. Nair, R. Balamurugan, J. Venugopal, W. Teo, J. Mater. Sci., 45 (2010) 6283-6312.

[25] Z. Ma, H. Ji, Y. Teng, G. Dong, J. Zhou, D. Tan, J. Qiu, J. Colloid. Interface. Sci., 358 (2011) 547-553.

[26] M.K. Sarkar, K. Bal, F. He, J. Fan, Appl. Surf. Sci., 257 (2011) 7003-7009.

[27] M. Ma, Y. Mao, M. Gupta, K.K. Gleason, G.C. Rutledge, Macromolecules, 38 (2005) 9742-9748.

[28] D. Li, J.T. McCann, Y. Xia, M. Marquez, J. Am. Ceram. Soc., 89 (2006) 1861-1869.

[29] M. Guo, B. Ding, X. Li, X. Wang, J. Yu, M. Wang, J. Phys. Chem. C, 114 (2009) 916-921.

[30] F. Zhao, X. Wang, B. Ding, J. Lin, J. Hu, Y. Si, J. Yu, G. Sun, RSC Advances, 1 (2011) 1482-1488.

[31] B. Ding, T. Ogawa, J. Kim, K. Fujimoto, S. Shiratori, Thin Solid Films, 516 (2008) 2495-2501.

[32] H.Z. Tang, H. Wang, J.H. He, J. Phys. Chem. C., 113 (2009) 14220-14224.

[33] L.Y. Meng, S. Han, N. Jiang, W. Meng, Mater. Chem. Phys., 148 (2014) 798-802.

[34] K. Nakane, M. Seto, S. Irie, T. Ogihara, N. Ogata, J. Appl. Polym. Sci., 121 (2011) 1774-1779.

[35] K. Nakane, S. Matsuoka, S. Gao, S. Yonezawa, J. Kim, N. Ogata, J. Min. Metall. Sect. B-Metall., 49 (2013) 77-82.

[36] Z. Zivkovic, N. Mitevska, I. Mihajlovic, D. Nikolic, J. Min. Metall. Sect. B-Metall., 45 (2009) 23-34.

[37] J. Purenovic, V.V. Mitic, V. Paunovic, M. Purenovic, J. Min. Metall. Sect. B-Metall., 47 (2011) 157-169.

[38] A. Cassie, S. Baxter, J. Chem. Soc. Faraday Trans., 40 (1944) 546-551.

[39] M. Miwa, A. Nakajima, A. Fujishima, K. Hashimoto, T. Watanabe, Langmuir, 16 (2000) 5754-5760.

[40] S. Haukka, A. Root, J. Phys. Chem., 98 (1994) 1695-1703.